Article

Synthesis of 5-(Hydroxymethyl)furfural Monoesters and Alcohols as Fuel Additives toward Their Performance and Combustion Characteristics in Compression Ignition Engines

Ob Nilaphai, Sukanya Thepwatee, Piriya Kaeopookum, Laksamee Chaicharoenwimolkul Chuaitammakit, Chonticha Wongchaichon, Onnicha Rodjang, Prapapron Pudsong, Wanida Singhapon, Thanakorn Burerat, Siriporn Kamtaw, Sathaporn Chuepeng, and Sopanat Kongsriprapan*

Read Online

ACCESS | Metrics & More | Article Recommendations | Supporting Information

ABSTRACT: The synthesis of 5-(hydroxymethyl)furfural (HMF) and conversion to the corresponding HMF-monoesters upon certain treatment are presented with their properties that are validated in a diesel engine. With a collection of fatty acids (C8−C18) using cyanuric acid as a catalyst under mild reaction conditions, the subsequent reduction of the HMF-monoesters with NaBH$_4$ produced the corresponding alcohols. After purification, both HMF-monoesters and their alcohol derivatives were determined for their solubility, cetane index, heat of combustion, viscosity, and specific gravity. HMF-Capric (**1-C10**), HMF-Oleic (**1-C18:1**), HMF-Caprylic-OH (**2-C8**), and HMF-Oleic-OH (**2-C18:1**) were soluble in a neat diesel fuel. The observed highest cetane index and heat of combustion of **1-C10** and **1-C18:1** were evaluated for combustion characteristics in a single-cylinder compression ignition engine. The diesel fuel containing 3% **1-C10** displayed comparable properties during burning in terms of thermal efficiency, cylinder pressure, and heat release rate with respect to the neat diesel fuel (D100) for all usage engine speeds. In general, all tested fuels initiated their burning onset with a similar ignition delay period. The 3% **1-C10**-blended diesel fuel emitted slightly higher smoke opacity but an equivalent nitric oxide level compared to those of D100. The HMF-Capric (**1-C10**) synthesized in this study represents a promising additive for diesel fuel. Blended fuel lubricity and other unregulated emissions upon broader engine test cycles are suggested to be accomplished in future work.
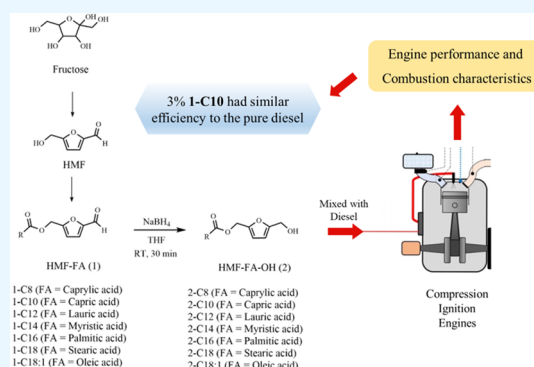
1. INTRODUCTION

In the global supply chain, diesel fuel has been progressively playing a vital role in developing economy particularly for the transportation sector and power generation for minority countries. Apart from public transport that has been transformed to electric-powered vehicles, other means of human and good logistics yet rely on diesel engine power.[1] As the global economy relentlessly rises, petroleum diesel is continuously consumed, resulting in its vast depletion, energy security, and environmental concerns.[2] These concerns have been sorted by establishing research schemes on production and utilization of renewable fuels.[3]

A range of biofuels have been receiving particular attention and have been actively disclosed in the past decades.[4] Biodiesel, one of the renewable fuels, is a sustainable and compatible diesel substitute that has been adapted to the global market.[5] Biodiesel can be blended with petroleum diesel at different concentrations with the most common maximum biodiesel blend being B30 (30% biodiesel and 70% petroleum diesel).[6] Biodiesel−petroleum diesel-blended fuels offer a high cetane number that causes improvements of particulate matter

and sulfur oxide emissions.[7] However, biodiesel blends containing greater than 30% biodiesel show certain limitations,[8] particularly poor cold flow properties.[9] In addition, edible plant as a feedstock for biodiesel production is yet of concern when biodiesel has to be substituted in a greater proportion into petroleum diesel.[10] Therefore, a quest for novel promising fuel additives is crucially required, especially oxygenated reagents that are beneficial in terms of environmentally friendly atmosphere and low friction energy.[11]

5-(Hydroxymethyl)furfural (HMF) is listed as a top value-added biobased compound required for a successful renewable economy by the United States Department of Energy.[12] HMF can be derived from cellulose and starch of biomass and can be transformed into high-value derivatives for a variety of
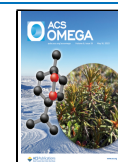
applications.[13] In energy applications, HMF has been used as a precursor for the synthesis of liquid fuels and fuel additives. 5-(Ethoxymethyl)furfural (EMF), an etherification product of HMF and ethanol, is identified as a potential diesel additive. It possesses high solubility in diesel and high energy density and is capable of reducing soot, sulfur oxide (SO_x), and nitrogen oxide (NO_x) emissions.[14,15] In addition, levulinic acid (LA), a dehydration product of HMF, can be converted to levulinic acid ester (LAE), which can be blended with diesel to improve cold flowability and reduce SO_x emissions.[16] Although EMF and LAE have demonstrated great potential as diesel additives, the complicated synthesis methods and harsh reaction conditions are the major challenges for commercialization.[17] Therefore, exploration of new additives conveniently prepared from a simple synthetic process has drawn attention to be disclosed.

Recently, the synthesis of 2,5-bis(hydroxymethyl)furan (BHMF) fatty acid (FA) diesters via enzymatic esterification of HMF-derived 2,5-bis(hydroxymethyl)furan (BHMF) with free fatty acids (FA) using Novozym 435 lipase has been disclosed.[17−19] Krystof and co-workers showed that HMF levulinate can be prepared by enzymatic esterification of HMF with levulinic acid using Novozym 435 lipase as an enzyme. However, the biocatalytic process generally requires a high production cost and a limited range of operating conditions.[20] Additionally, the product yields could be suppressed with increasing reactant concentration or reaction temperature.[21,22]

In the aspect of catalysts for production of HMF, several research groups reported novel catalysts that yielded a high percentage of conversion of biomass to HMF. Malkar et al. reported an aluminum-exchanged heteropolyacid with the maximum conversion of 99% biomass to HMF within 10 h. This four-time reusable catalyst was stable and able to form C9 adducts at up to 84%.[23] Hafizi and co-workers were successful in the synthesis of a Lewis/Brønsted catalyst of sulfated bimetallic $SO_4^{2−}$/Al-Zr/KIT-6. This synthesized acid hybrid nanocatalyst was efficient and environmentally friendly that can yield 89.8% EMF and HMF conversion of 99% from biomass.[24] Elsayed et al. developed a low-cost ZnO-Fe_3O_4/AC bimetallic nanocatalyst that can be recycled up to five times. Through two-step sequential selective hydrogenation and etherification reactions of HMF to BHMF, the yields were converted into biofuel additives such as alkoxymethylfurans (AMFs) and 2,5-bis(alkoxymethyl)furans (BAMFs) using Brønsted acid catalysts. The AMFs and BAMFs were attained at over 85% at the end of the etherification reaction.[25] Tonutti et al. compared the performance of the synthesized mesoporous silica catalysts between MCM-41 and SBA-15 in terms of the sulfonic acid site ($-O_3H$) amount at 140 °C. After four reaction cycles, the catalyst still possessed its activity by reaching 78% HMF conversion and 68.7% EMF yield.[26]

By reviewing the studies in all points of view, to bridge research gaps, an exploration of a new and mild chemical catalytic process to synthesize HMF-monoesters to be used as diesel additives is initiated. In addition, research on the synthesized HMF fuel additives validated in real usage conditions of diesel engines was rarely seen; only few cases have been reported for combustion and emission characteristics.[27−29] Therefore, for the objectives of this study, the starting HMF was prepared and then esterified with different-chain length free fatty acids (C8−C18) using cyanuric chloride as a catalyst. A series of esters, HMF-FA, and the reduced form, HMF-FA-OH, were synthesized, identified, and

evaluated for their properties with a diesel engine. A novel chemical catalytic synthesis of HMF-monoesters from HMF and free fatty acids will be described and discussed with the suggestion of further steps of development.

2. EXPERIMENTAL APPARATUS AND METHODOLOGIES

2.1. General. All chemical reagents of analytical grade from Merck Millipore (Darmstadt, Germany) and TCI (Tokyo, Japan) were used without prepurification. Ultralow-sulfur diesel (ULSD) was received from PTT Global Chemical Public Co. Ltd. (Bangkok, Thailand).

Nuclear magnetic resonance (NMR) spectroscopy was employed for the characterization of HMF and its derivatives. All solid samples were collected at melting temperature using a METTLER TOLEDO (Melting Point System MP30). ^1H and ^{13}C NMR spectra were recorded on a Bruker AVANCE 400 (400 MHz) spectrometer (Bruker, Massachusetts). Chemical shifts (δ) were reported in parts per million (ppm) relative to an internal standard, tetramethylsilane (TMS) ($\delta = 0$), for ^1H NMR or residual nondeuterated solvent peaks for ^{13}C NMR.

2.2. Synthesis of HMF. In a round-bottom flask, D-fructose (1.5 g, 8.3 mmol) was dissolved in 0.25 M HCl (30 cm^3). The solution was heated at 115 °C for 30 min using an Environmental Express HotBlock digestor. Thereafter, the mixture was extracted with dichloromethane (3 × 30 cm^3). The combined organic phase was washed with water (3 × 30 cm^3) and saturated sodium chloride (sat. NaCl) (1 × 30 cm^3) and dried over anhydrous sodium sulfate (anh. Na$_2$SO$_4$). After removal of the solvent under reduced pressure, HMF was obtained.

2.3. Synthesis of HMF-FA (1). The starting HMF-FA (1) was synthesized under modified conditions by following the literature.[30] HMF (5.0 g, 40.0 mmol) was reacted with 44.0 mmol fatty acid (FA), caprylic acid (C8), capric acid (C10), lauric acid (C12), myristic acid (C14), palmitic acid (C16), stearic acid (C18), or oleic acid (C18:1), in toluene (300 cm^3) using triethylamine (NEt$_3$) as a base and cyanuric chloride (8.1 g, 44.0 mmol) as a catalyst, detailed in the equation for the quantitative analysis of reaction mixtures in the Supporting Information (SI). The mixture was heated at 100 °C overnight. Then, the reaction mixture was filtered by vacuum filtration and washed with ethyl acetate. After solvent removal (in vacuo), the residue was separated by column chromatography using silica gel as a stationary phase and ethyl acetate/hexane as a mobile phase. The purified products were denoted as HMF-FA (**1**), HMF-Caprylic (**1-C8**), HMF-Capric (**1-C10**), HMF-Lauric (**1-C12**), HMF-Myristic (**1-C14**), HMF-Palmitic (**1-C16**), HMF-Stearic (**1-C18**), and HMF-Oleic (**1-C18:1**).

2.4. Reduction of HMF-FA to HMF-FA-OH (2). To a 100 cm^3 tetrahydrofuran (THF) solution of HMF-FA (40.0 mmol), sodium borohydride (NaBH$_4$, 60.0 mmol) in THF (10 cm^3) was added dropwise. After stirring at room temperature (RT) for 30 min, the reaction was diluted with deionized water (50 cm^3). The resulting mixture was extracted with ethyl acetate (3 × 50 cm^3). The combined organic phase was washed with water (3 × 30 cm^3) and saturated NaCl (1 × 30 cm^3) and dried over anhydrous Na$_2$SO$_4$. After solvent removal, the crude product was purified by column chromatography using the same procedure as described in Section 2.3. The obtained products were represented as HMF-FA-OH (**2**), HMF-Caprylic-OH (**2-C8**), HMF-Capric-OH (**2-**
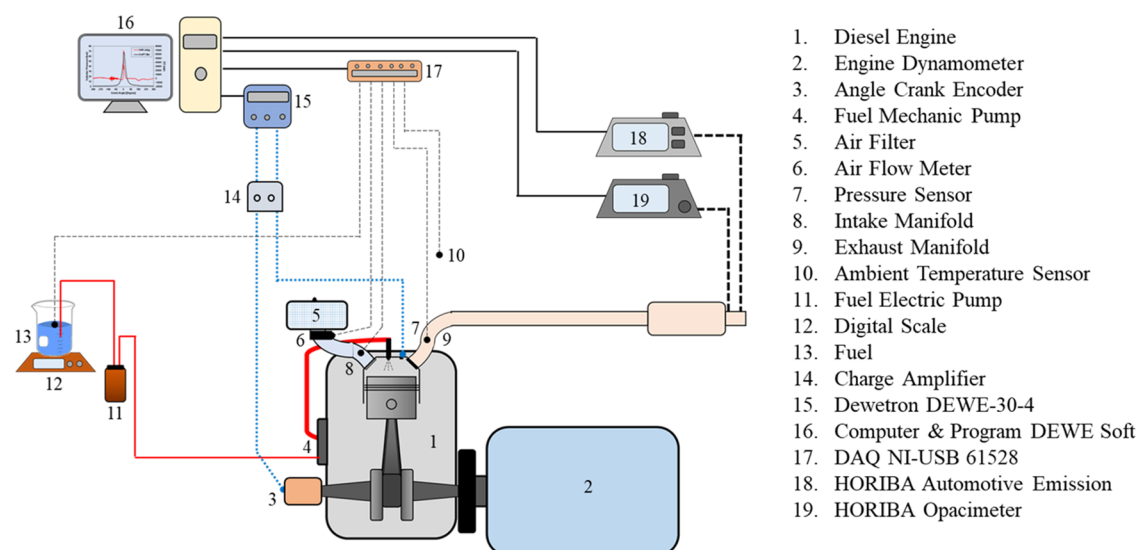
Figure 1. Schematic diagram of the engine test of diesel blends HMF-FA (**1**) and HMF-FA-OH (**2**).

C10), HMF-Lauric-OH (**2-C12**), HMF-Myristic-OH (**2-C14**), HMF-Palmitic-OH (**2-C16**), HMF-Stearic-OH (**2-C18**), and HMF-Oleic-OH (**2-C18:1**).

2.5. Analytical Part. The expected product purified by column chromatography was balanced by gravimetric analysis and calculated comparing with HMF-FA. All products were collected by ^{1}H and ^{13}C NMR spectroscopy. Each sample was dissolved in chloroform-*d* and filled in an NMR tube. The NMR spectrum was recorded in a chemical shift range of 0−12 ppm.

2.6. Solubility in Diesel Fuel. Solubility in diesel of HMF-FA (**1**) and the reduced form HMF-FA-OH (**2**) was evaluated by mixing the sample (0.1 g) with commercial diesel oil (0.5 cm^3) under stirring conditions (1500 rpm) for 10 min at RT. Homogeneity of the mixture was visually observed and considered "soluble" if a clear solution was achieved.

2.7. Determination of Engine Performance and Combustion Characteristics. Diesel blend fuels with additives HMF-FA (**1**) or HMF-FA-OH (**2**) were investigated for compatibility with the engine performance. To investigate the effect of fuels on the engine combustion characteristics, a single-cylinder diesel engine, Kubota RT100, was used and installed with an engine dynamometer to control the engine load and speed, as illustrated in Figure 1. The engine specifications are listed in Table 1. In this work, the engine was run at speeds of 1400, 1500, and 1600 rpm and the engine load was controlled using the engine dynamometer at 4.0 bars of indicated mean effective pressure (IMEP), which is the usual operating range of the application. It can be determined

by dividing the output work in a cycle by swept volume of the engine, expressed by

$$IMEP = \frac{1}{V_d} \int_0^{720} p \, dV \tag{1}$$

where V_d is the swept volume of the engine, p is the cylinder pressure (CP), and V is the cylinder volume. A piezoelectric dynamic sensor, Kistler model 6052C, with a linearity of ±0.4% full scale output was installed at the middle of the combustion chamber to measure the dynamic pressure and analyze the combustion characteristics. The pressure signal was filtered and amplified using a charge amplifier, Dewetron, model DEWE-30-4. The volume of the combustion chamber at different crank angle positions was detected using an incremental shaft encoder, Baumer Electric, model BDK 16.05A360-5-4, with 1° crank angle of resolution (360 pulses per revolution). The cylinder pressure (CP) and crank angle signals were recorded using a data acquisition system (DAQ), Dewetron, model DEWE-ORION-0816-100x.

Due to the energy output being controlled using the engine dynamometer, the fuel consumption was considered the energy input to compare the effects of fuels on engine performance. It can be defined as the mass flow rate of fuel ($\dot{m}_f$) consumed during engine operation and measured using a digital weight scale (CST, model CDR-3) at ±0.05-g accuracy. To investigate the efficiency of fuel conversion from chemical energy to engine power,[31] the thermal efficiency (η_{th}) was calculated according to the equation

$$\eta_{th} = \frac{P_b}{\dot{m}_f \times LHV} \tag{2}$$

where LHV is the lower heating value of the fuel and P_b is the power output measured by the engine dynamometer. Generally, the heat release rate (HRR) is used to analyze and characterize the combustion behavior of fuels in the combustion chamber.[32] It can be determined by the variation of cylinder pressure and volume in different crank angles, as expressed by the relation

$$HRR = \frac{\gamma}{\gamma - 1} p \frac{dV}{d\theta} + \frac{1}{\gamma - 1} V \frac{dp}{d\theta} \tag{3}$$

Table 1. Specifications of the Engine for the Test of Performance and Combustion Characteristics

specifications	details[33]
engine model	Kubota RT100
injection/cooling system	direction injection/water-cooled system
bore × stroke	88 mm × 90 mm
swept volume	547.0 cm^3
compression ratio	22:1
max. torque	33.4 N m at 1400 rpm
max. power	7.4 kW at 2400 rpm

where γ is the specific heat ratio, θ is the position of the crank angle, and V is the cylinder volume. To examine the effect of fuel properties on the exhaust gas emissions, a gaseous emission analyzer (Horiba Automotive Emission, model MEXA-584L) and a smoke meter (Horiba Opacimeter, model MEXA-130S) were equipped to measure the nitric oxide (NO) and the black smoke at the engine tail pipe, respectively.

Generally, the combustion process of the direct-injection diesel engine (Figure 2) is mainly composed of three phases
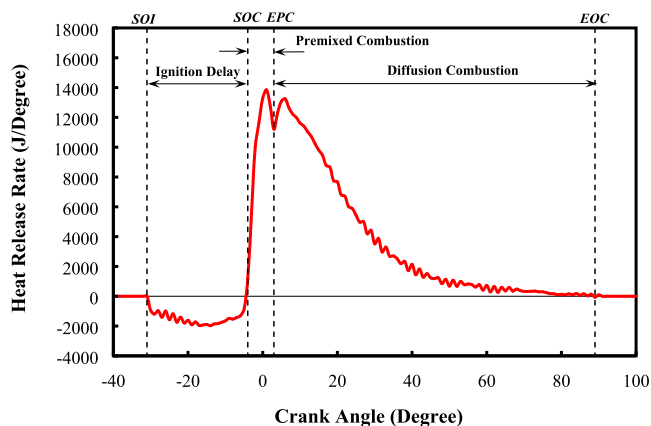
Figure 2. Combustion process of the direct-injection diesel engine.

(Nilaphai and Chuepeng, 2022).[33] It can be classified by using the heat release rate data. The first phase is called ignition delay (ID), presenting the autoignition ability of fuels and depending on the cetane number and ambient conditions in the combustion chamber such as temperature, pressure, and density.

The ignition delay is characterized by the time period from the start of injection (SOI) to the start of combustion (SOC). The SOI can be determined by the time where the heat in the combustion chamber was absorbed during the fuel vaporization process; the HRR profile turns to a negative value. On the other hand, the SOC is where the HRR returns to a positive value due to the beginning of the combustion process.[34] The second phase is called the premixed combustion; the HRR is rapidly increased due to the combustion of the accumulated air–fuel mixture in the ignition delay period. This period is defined as the time between the SOC and the end of premixed combustion

(EPC), where the end of the first heat release rate peak is. In the last phase, the HRR rises in the second peak by diffusive combustion, controlled by the injection rate and fuel vapor–air mixing. The end of combustion (EOC) in the last phase is defined as the time where the HRR returns to zero in the expansion stroke.

3. RESULTS AND DISCUSSION

3.1. Chemical Synthesis. HMF was synthesized via dehydration of D-fructose in aqueous solution catalyzed by HCl (Figure 3). The chemical structure of HMF was confirmed by ^{1}H and ^{13}C NMR spectroscopy (see the Supporting Information) receiving in 19% yield by qNMR analysis, and it was used as a starting material in the next step. The low yield observed may be attributed to the difficulty of dehydration of fructose. Next, HMF was esterified with various free fatty acids varying in carbon chain length (C8–C18) using cyanuric chloride as a catalyst under mild reaction conditions as shown in Figure 3. The esterified products HMF-FA (**1**) were obtained in moderate yields (44–51% yields) and characterized by ^{1}H and ^{13}C NMR spectroscopy (see the Supporting Information (SI)). The physical characteristics and yields of HMF-FA (**1**) are summarized in Table 2. Among all ester products, only HMF-Caprylic (**1-C8**), HMF-Capric (**1-C10**), and HMF-Oleic (**1-C18:1**) appeared as liquid at room temperature. HMF-monoesters, **1-C10** and **1-C18:1**, were chosen for evaluation of diesel additive properties due to their solubility in diesel (Figure S31, Supporting Information (SI)).

The aldehyde functional group of HMF-FA (**1**) can be converted into the hydroxyl group upon reduction using NaBH$_4$ as a reducing agent, resulting in HMF-FA-OH (**2**). This reduction step required a short reaction time (30 min) and gave high yields of HMF-FA-OH (**2**) in a range of 75–88%. This may arise from the solubility of the starting HMF-FA (**1**) in THF. The physical appearance and yields of HMF-FA-OH (**2**) are summarized in Table 2. It was found that only **2-C8** and **2-C18:1** are liquid and soluble in diesel at room temperature (see Figure S32, Supporting Information (SI)). The properties of the soluble compounds blended with diesel fuel were next investigated.

3.2. Properties of Diesel Blended with HMF-FA and HMF-FA-OH. Fuel properties of pure diesel (D100) and diesel blended with **1-C10**, **1-C18:1**, **2-C8**, and **2-C18:1** at the concentrations of 3 and 5% (w/v) are depicted in Table 3. The results indicated that all the blended diesels met the standard specification for diesel fuel. These findings supported the
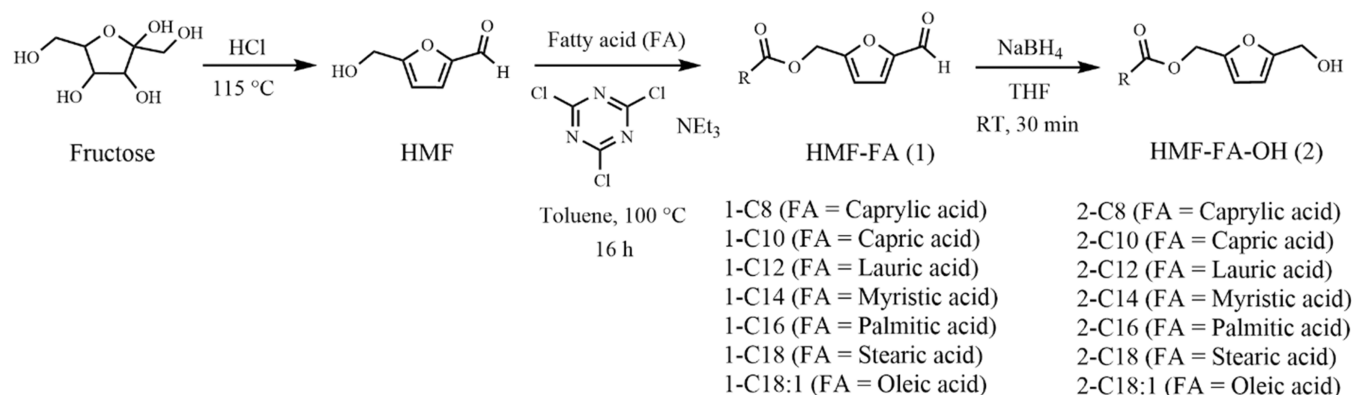
Figure 3. Synthesis of HMF-FA-OH (**2**) alcohols from D-fructose via HMF and HMF-FA (**1**) ester of various fatty acids.

Table 2. Chemical Yields and Characteristics of HMF-FA (1) and HMF-FA-OH (2)[a]

Product name	Fatty acid	Product	Appearance	Soluble in diesel	Yield[a] (%)
1-C8	Caprylic acid (C8)		yellow liquid	×	46
1-C10	Capric acid (C10)		yellow liquid	/	50
1-C12	Lauric acid (C12)		yellow solid	×	48
1-C14	Myristic acid (C14)		yellow solid	×	44
1-C16	Palmitic acid (C16)		yellow solid	×	51
1-C18	Stearic acid (C18)		yellow solid	×	47
1-C18:1	Oleic acid (C18:1)		yellow liquid	/	49
2-C8	Caprylic acid (C8)		light yellow liquid	/	75
2-C10	Capric acid (C10)		light yellow liquid	×	81
2-C12	Lauric acid (C12)		light yellow solid	×	88
2-C14	Myristic acid (C14)		light yellow solid	×	82
2-C16	Palmitic acid (C16)		light yellow solid	×	83
2-C18	Stearic acid (C18)		light yellow solid	×	82
2-C18:1	Oleic acid (C18:1)		light yellow liquid	/	84
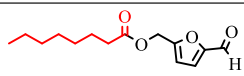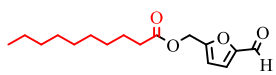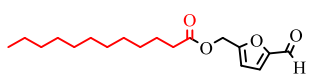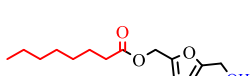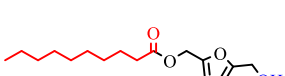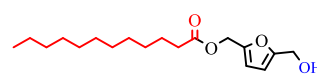
[a]Gravimetric yield.

feasibility of **1-C10**, **1-C18:1**, **2-C8**, and **2-C18:1** as potential diesel additives. For further test in a diesel engine, diesels blended with ester, 3% HMF-Capric (3% **1-C10**) and 3% HMF-Oleic (3%**1-C18:1**) fuels (see Figure S33, Supporting Information (SI)), were selected due to their highest cetane number and heat of combustion, respectively.

3.3. Engine Performance. The engine performance in terms of fuel consumption and thermal efficiency at 4.0 bar

IMEP and varied engine speeds from 1400 to 1600 rpm is illustrated in Figure 4. The fuel consumption of both 3% **1-C10** and 3% **1-C18:1** was slightly enhanced by increasing the engine speed. More fuel was injected in the combustion chamber to achieve higher engine speeds. At lower engine speeds, 3% **1-C10** presented the lowest fuel consumption followed by D100 and 3% **1-C18:1**. However, at the highest engine speed, 1600 rpm, the fuel consumption of 3% **1-C10**

Table 3. Fuel Properties of Diesel Blended with HMF-FA (1) and HMF-FA-OH (2)

fuel	cetane index	heat of combustion (MJ/kg)	viscosity at 40 °C (cSt)	specific gravity at 15 °C (60 °F)
standard method	ASTM D 976	ASTM D 240	ASTM D 445	ASTM D 4052
standard value	≥50		1.8−4.1	0.81−0.87
diesel (D100)	53.5	46.5	2.681	0.8260
3% **1-C10**	53.0	46.5	2.632	0.8296
5% **1-C10**	50.0	44.0	2.656	0.8335
3% **1-C18:1**	51.0	47.1	2.740	0.8309
5% **1-C18:1**	51.0	45.3	2.751	0.8312
3% **2-C8**	51.0	46.1	2.708	0.8297
5% **2-C8**	49.5	46.0	2.672	0.8331
3% **2-C18:1**	52.0	46.0	2.689	0.8296
5% **2-C18:1**	52.0	45.4	2.821	0.8315
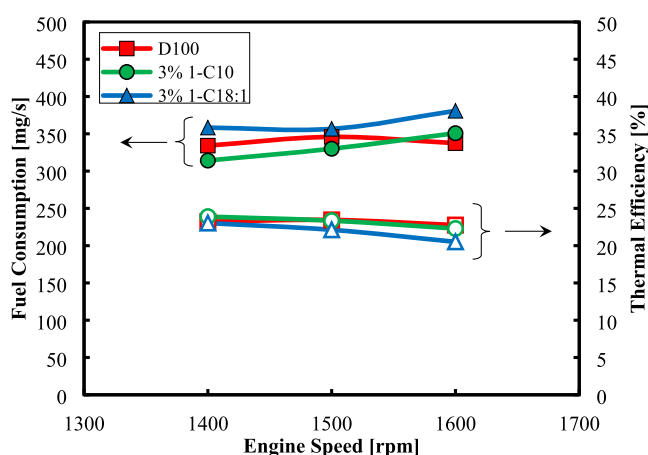
Figure 4. Engine performance in terms of fuel consumption and thermal efficiency of pure diesel (D100) and diesel blends: 3% **1-C10** and 3% **1-C18:1**.

was pronounced to the higher level than that of D100. The 3% **1-C18:1** was found to present the highest fuel consumption at any speed levels. The findings related to the fuel properties are shown in Table 3. The 3% **1-C10** expressed the similar heat of combustion, cetane number, specific gravity, and viscosity to D100. Therefore, its fuel consumption was comparable to that of D100 for all test conditions. On the other hand, even though the 3% **1-C18:1** offered higher heat of combustion than that of D100, its specific gravity and viscosity were greater than those of D100. Generally, the higher values of specific gravity and viscosity prohibit the spray and atomization development, for example, a long liquid and vapor spray penetration and poor fuel atomization can cause the incompletion of fuel combustion.[35] As a result, the higher fuel consumption of 3% **1-C18:1** compared to that of 3% **1-C10** and D100 was observed. This assumption was emphasized by the thermal efficiency as displayed in Figure 4. The 3% **1-C10** exhibited similar thermal efficiency to that of D100 at all test speeds, whereas the 3% **1-C18:1** revealed the lowest one.

3.4. Fuel Combustion Characteristics. The combustion characteristics and autoignition ability of the pure and blended diesel fuels tested in a single-cylinder diesel engine are demonstrated in Figures 5 and 6, respectively. The cylinder pressure and heat release rate (HRR) profiles were in the same trend for all tested fuels, possibly due to their insignificant difference in fuel properties. As shown in Figure 5 (left axis), the cylinder pressure profiles started to rise during compression stroke and then quickly increased at −6, −5,
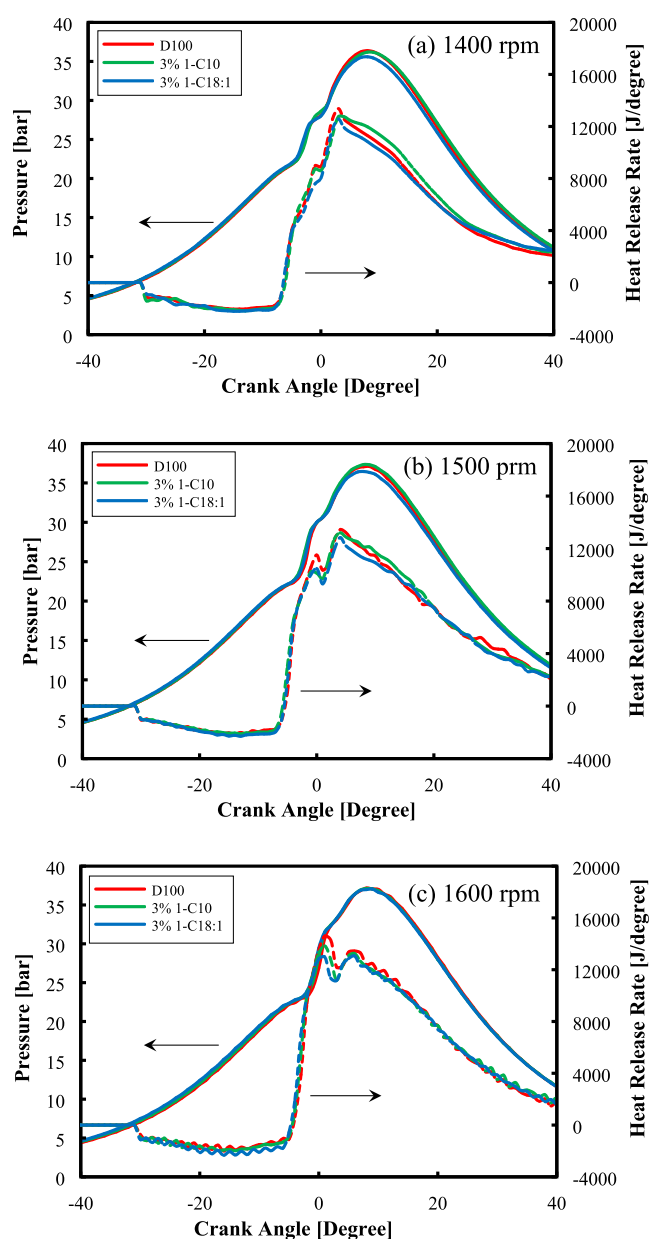
Figure 5. Cylinder pressure and heat release rate of diesel (D100), 3% **1-C10**, and 3% **1-C18:1** at the engine speeds of (a) 1400 rpm, (b) 1500 rpm, and (c) 1600 rpm.

and −4 before the top dead center (bTDC) for 1400, 1500, and 1600 rpm, respectively, due to the start of fuel combustion.
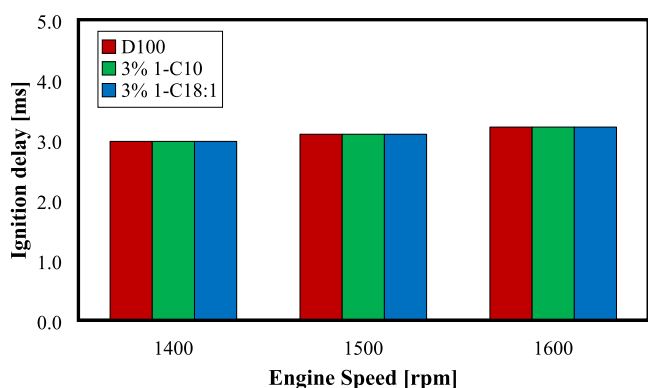
Figure 6. Ignition delay of diesel (D100), 3% **1-C10**, and 3% **1-C18:1** at the engine speeds of 1400, 1500, and 1600 rpm.

After that, it dramatically increased again to reach the maximum pressure by the premixed combustion process. Comparison to D100, the 3% **1-C10** exhibited similar profiles for the whole cycle at all engine speeds, while 3% **1-C18:1** revealed a slightly lower maximum pressure around the top dead center (TDC) at the engine speeds of 1400 and 1500 rpm.

The HRR profiles started to decrease and were found in the negative value range at 31° before the top dead center (bTDC) for all test conditions, presenting the timing of the fuel injected into the combustion chamber. Then, they returned to positive values at around 4−6° bTDC due to the started fuel combustion. This period showed the heat loss during the vaporization process, which is generally found in direct-injection diesel engines.[32] The heat around the combustion chamber is induced to entrain the fuel injected into the combustion chamber in the vaporization process.[34] This period also indicates the autoignition ability of fuel in terms of the ignition delay as explained in the experimental part (Section 2.7). As can be seen in Figure 6, all tested fuels expressed equivalent ignition delay, which was slightly higher with increasing engine speeds. This equality was a result of their comparable cetane index.

After the start of the combustion period, the HRR increased to the maximum value at around the TDC and then slowly fell in the expansion stroke. As observed, the maximum HRR of the 3% **1-C10** was closer to that of D100 than that of the 3% **1-C18:1** due to its approximate fuel properties. This is in accordance with the assumption discussed in the engine performance part (Section 2.7); the 3% **1-C18:1** has the poorest combustion efficiency compared to D100 and 3% **1-C10**, as it presented the highest specific gravity and viscosity and lowest cetane index.

To investigate the effect of fuel properties on combustion characteristics, the accumulated heat in different combustion phases is presented Figure 7. In the first period, ignition delay, the heat release with a negative value presents a similar level for all testing conditions, related to the level of ignition delay and CN, while there is no effect of fuel properties on the premixed combustion phase, as shown by the same level of accumulated heat when compared at the same engine speed. However, it increases with higher engine speeds because the high surrounding heat at the high engine speed enhances the autoignition and premixed combustion process. At the last period of combustion, the 3% **1-C10** presents the highest heat release for all engine speeds. This is due to the highest level of
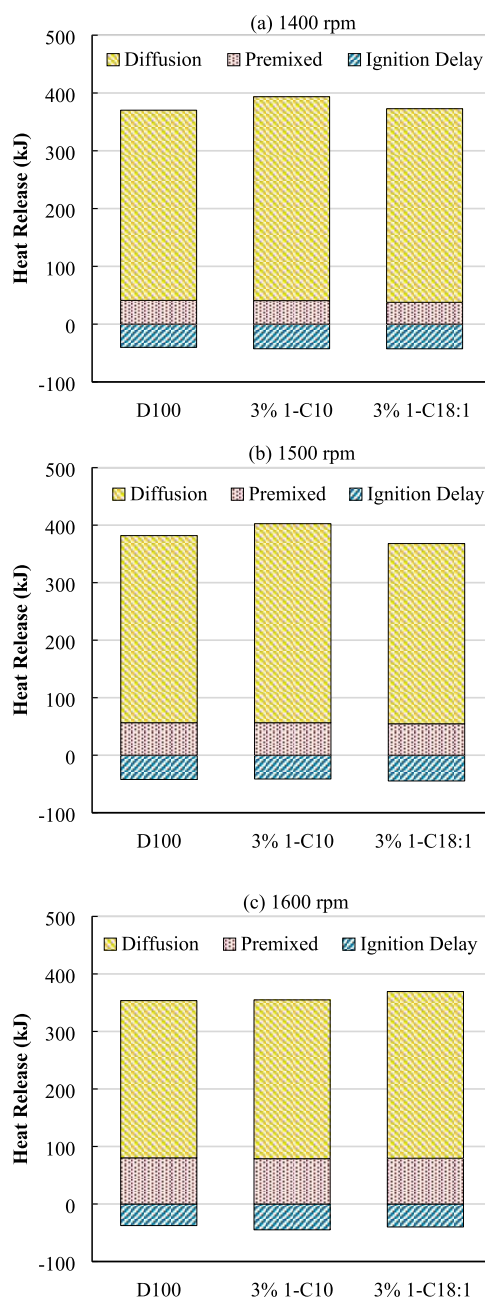
Figure 7. Combustion phase of diesel (D100), 3% **1-C10**, and 3% **1-C18:1** at the engine speeds of (a) 1400, (b) 1500, and (c) 1600 rpm.

oxygen contained in its molecule at 22.86% by weight, which is higher than that of diesel and 3% **1-C18:1** at 0 and 16.41% by weight, respectively. The high oxygen present promotes the oxidation of the air−fuel mixture, which emphasizes that the small amount of 3% **1-C18:1** can promote the combustion process, especially in the diffusive combustion phase.

In Figure 8, nitric oxide (NO) and smoke emission profiles for all tested fuels at 4 bar IMEP with different engine speeds are displayed. The exhaust gas emissions showed good agreement with the engine performance and combustion behavior. The low engine performance and poor combustion efficiency of the 3% **1-C18:1** caused higher smoke opacity and lower NO emission compared to those of the other fuels. The trade-off between NO_x and smoke emissions is normally found in diesel engines.[36] On the contrary, the 3% **1-C10** displayed a
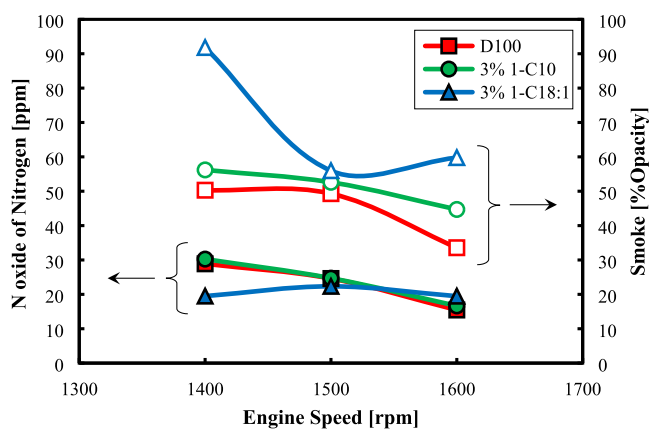
Figure 8. Exhaust gas emissions, nitric oxide, and smoke of pure diesel, 3% **1-C10**, and 3% **1-C18:1**.

great potential to be applied in diesel engines, as it revealed a similar level of NO emission but only a slight increase of smoke emission compared to that of D100 for all test conditions.

4. CONCLUSIONS

This work demonstrates a novel catalytic synthesis method of HMF-monoesters from fatty acids using cyanuric acid as a catalyst. The isolated HMF-monoesters and alcohols were tested for their solubility in a commercial diesel fuel. HMF-Capric (**1-C10**), HMF-Oleic (**1-C18:1**), HMF-Caprylic-OH (**2-C8**), and HMF-Oleic-OH (**2-C18:1**) were completely soluble in the diesel fuel. According to the highest cetane index of the **1-C10** and heat of combustion of the **1-C18:1**, they were blended with the diesel fuel and tested with a single-cylinder diesel engine. The diesel blended with 3% **1-C10** had similar fuel combustion, thermal efficiency, cylinder pressure, and heat release rate to those of the pure diesel (D100) at all engine speeds: 1400, 1500, and 1600 rpm. It also exhibited a comparable NO emission profile but a slightly higher smoke opacity compared to those of D100. On the contrary, the diesel blended with 3% **1-C18:1** showed a relatively higher fuel consumption, lower thermal efficiency, and lower heat release rate at higher engine speeds. The NO emission profile was slightly increased with increasing engine speeds. The significant reduction of smoke opacity was observed at 1400 rpm. In terms of the ignition delay, there was no significant change for both blended fuels. These findings showed the feasibility of a new synthesis method for HMF-monoesters and their potential use for diesel engines.

■ ASSOCIATED CONTENT

ⓢ Supporting Information

The Supporting Information is available free of charge at https://pubs.acs.org/doi/10.1021/acsomega.3c02385.

Color and state of products, melting point of solid products, ^{1}H and ^{13}C NMR, solubility, appearance of pure diesel and the blended diesels, equation of the quantitative analysis of reaction mixtures, and yield calculation of the product (PDF)

■ AUTHOR INFORMATION

Corresponding Author

Sopanat Kongsriprapan − *Department of Basic Science and Physical Education, Faculty of Science at Sriracha, Kasetsart University, Tung Sukla, Chon Buri 20230, Thailand;* ⓞ orcid.org/0000-0001-6433-3451; Phone: +66 3835 4580; Email: sfscispk@ku.ac.th; Fax: +66 3835 4587

Authors

Ob Nilaphai − *ATAE Research Unit, Department of Mechanical Engineering, Faculty of Engineering at Sriracha, Kasetsart University, Thung Sukhla, Chon Buri 20230, Thailand*

Sukanya Thepwatee − *Department of Industrial Chemistry, Faculty of Applied Science, King Mongkut's University of Technology North Bangkok, Bangkok 10800, Thailand*

Piriya Kaeopookum − *Nuclear Technology Research and Development Center, Thailand Institute of Nuclear Technology, Ongkarak, Nakhon Nayok 26120, Thailand*

Laksamee Chaicharoenwimolkul Chuaitammakit − *Chemistry, Faculty of Science and Technology, Suratthani Rajabhat University, Surat Thani 84100, Thailand*

Chonticha Wongchaichon − *Department of Basic Science and Physical Education, Faculty of Science at Sriracha, Kasetsart University, Tung Sukla, Chon Buri 20230, Thailand*

Onnicha Rodjang − *Department of Basic Science and Physical Education, Faculty of Science at Sriracha, Kasetsart University, Tung Sukla, Chon Buri 20230, Thailand*

Prapapron Pudsong − *Department of Basic Science and Physical Education, Faculty of Science at Sriracha, Kasetsart University, Tung Sukla, Chon Buri 20230, Thailand*

Wanida Singhapon − *Department of Basic Science and Physical Education, Faculty of Science at Sriracha, Kasetsart University, Tung Sukla, Chon Buri 20230, Thailand*

Thanakorn Burerat − *ATAE Research Unit, Department of Mechanical Engineering, Faculty of Engineering at Sriracha, Kasetsart University, Thung Sukhla, Chon Buri 20230, Thailand*

Siriporn Kamtaw − *ATAE Research Unit, Department of Mechanical Engineering, Faculty of Engineering at Sriracha, Kasetsart University, Thung Sukhla, Chon Buri 20230, Thailand*

Sathaporn Chuepeng − *ATAE Research Unit, Department of Mechanical Engineering, Faculty of Engineering at Sriracha, Kasetsart University, Thung Sukhla, Chon Buri 20230, Thailand;* ⓞ orcid.org/0000-0001-8613-0233

Complete contact information is available at:
https://pubs.acs.org/10.1021/acsomega.3c02385

Author Contributions

O.N.: conceptualization, methodology, validation, formal analysis, investigation, writing—original draft, and visualization. S.T.: writing—original draft. P.K.: writing—reviewing and editing. L.C.C.: writing—reviewing and editing. C.W.: investigation. O.R.: investigation. P.P.: investigation. W.S.: investigation. T.B.: investigation. S.K.: investigation. S.C.: research design, data analysis, conclusion, recommendation, writing—reviewing and editing, and supervision. S.K.: conceptualization, methodology, investigation, writing—original draft, supervision, and project administration.

Notes

■ ACKNOWLEDGMENTS

■ REFERENCES

(1) Kebede, L.; Tulu, G. S.; Lisinge, R. T. Diesel-fueled public transport vehicles and air pollution in Addis Ababa, Ethiopia: Effects of vehicle size, age and kilometers travelled. *Atmos. Environ.: X* **2022**, *13*, No. 100144.

(2) Abas, N.; Kalair, A.; Khan, N. Review of fossil fuels and future energy technologies. *Futures* **2015**, *69*, 31−49.

(3) Alipour, S.; Omidvarborna, H.; Kim, D.-S. A review on synthesis of alkoxymethyl furfural, a biofuel candidate. *Renewable Sustainable Energy Rev.* **2017**, *71*, 908−926.

(4) Nakagawa, Y.; Tamura, M.; Tomishige, K. Recent development of production technology of diesel- and jet-fuel-range hydrocarbons from inedible biomass. *Fuel Process. Technol.* **2019**, *193*, 404−422.

(5) Singh, D.; Sharma, D.; Soni, S. L.; Sharma, S.; Sharma, P. K.; Jhalani, A. A review on feedstocks, production processes, and yield for different generations of biodiesel. *Fuel* **2020**, *262*, No. 116553.

(6) Chuepeng, S.; Xu, H. M.; Tsolakis, A.; Wyszynski, M. L.; Price, P.; Stone, R.; Hartland, J. C.; Qiao, J. In *Particulate Emissions from a Common Rail Fuel Injection Diesel Engine with RME-based Biodiesel Blended Fuelling Using Thermo-gravimetric Analysis*, SAE Technical Paper, 2008.

(7) Thitipatanapong, S.; Visuwan, P.; Komintarachat, C.; Theinnoi, K.; Chuepeng, S. Insight into nanoparticle-number-derived characteristics of precharged biodiesel exhaust gas in nonthermal plasma state. *ACS Omega* **2022**, *7*, 5376−5384.

(8) Dangsunthonchai, M.; Visuwan, P.; Komintarachat, C.; Theinnoi, K.; Chuepeng, S. Nanoparticle components and number−size distribution of waste cooking oil-based biodiesel exhaust gas from a diesel particulate filter-equipped engine. *ACS Omega* **2022**, *7*, 3384−3394.

(9) Komintarachat, C.; Chuepeng, S. Catalytic enhancement of calcium oxide from green mussel shell by potassium chloride impregnation for waste cooking oil-based biodiesel production. *Bioresour. Technol. Rep.* **2020**, *12*, No. 100589.

(10) Komintarachat, C.; Chuepeng, S. Methanol-based trans-esterification optimization of waste used cooking oil over potassium hydroxide catalyst. *Am. J. Appl. Sci.* **2010**, *7*, 1073−1078.

(11) Kumwannaboon, W.; Chuepeng, S.; Komintarachat, C. Triacetin as lubricant additive: Slipping friction between metal pairs under boundary lubrication. *Appl. Sci. Eng. Prog.* **2023**, *16*, 5551−5563.

(12) Hu, L.; He, A.; Liu, X.; Xia, J.; Xu, J.; Zhou, S.; Xu, J. Biocatalytic transformation of 5-hydroxymethylfurfural into high-value derivatives: Recent advances and future aspects. *ACS Sustainable Chem. Eng.* **2018**, *6*, 15915−15935.

(13) Zhao, P.; Cui, H.; Zhang, Y.; Zhang, Y.; Wang, Y.; Zhang, Y.; Xie, Y.; Yi, W. Synergetic effect of Brønsted/Lewis acid sites and water on the catalytic dehydration of glucose to 5-hydroxymethylfurfural by heteropolyacid-based ionic hybrids. *ChemistryOpen* **2018**, *7*, 824−832.

(14) Balakrishnan, M.; Sacia, E. R.; Bell, A. T. Etherification and reductive etherification of 5-(hydroxymethyl)furfural: 5-(alkoxymethyl)furfurals and 2,5-bis(alkoxymethyl)furans as potential bio-diesel candidates. *Green Chem.* **2012**, *14*, 1626−1634.

(15) Lanzafame, P.; Papanikolaou, G.; Barbera, K.; Centi, G.; Perathoner, S. Etherification of HMF to biodiesel additives: The role of NH_4^+ confinement in Beta Zeolites. *J. Energy Chem.* **2019**, *36*, 114−121.

(16) Climent, M. J.; Corma, A.; Iborra, S. Conversion of biomass platform molecules into fuel additives and liquid hydrocarbon fuels. *Green Chem.* **2014**, *16*, 516−547.

(17) Quereshi, S.; Ahmad, E.; Pant, K. K.; Dutta, S. Synthesis and characterization of zirconia supported silicotungstic acid for ethyl levulinate production. *Ind. Eng. Chem. Res.* **2019**, *58*, 16045−16054.

(18) Lăcătuş, M. A.; Dudu, A. I.; Bencze, L. C.; Katona, G.; Irimie, F.-D.; Paizs, C.; Tosa, M. I. Solvent-Free Biocatalytic Synthesis of 2,5-bis-(Hydroxymethyl)Furan Fatty Acid Diesters from Renewable Resources. *ACS Sustainable Chem. Eng.* **2020**, *8*, 1611−1617.

(19) Lăcătuş, M. A.; Bencze, L. C.; Toşa, M. I.; Paizs, C.; Irimie, F.-D. Eco-Friendly Enzymatic Production of 2,5-Bis(hydroxymethyl)-furan Fatty Acid Diesters, Potential Biodiesel Additives. *ACS Sustainable Chem. Eng.* **2018**, *6*, 11353−11359.

(20) Krystof, M.; Pérez-Sánchez, M.; Domínguez de María, P. Lipase-catalyzed (trans)esterification of 5-hydroxy-methylfurfural and separation from HMF esters using deep-eutectic solvents. *ChemSusChem* **2013**, *6*, 630−634.

(21) Qin, Y.-Z.; Zong, M.-H.; Lou, W.-Y.; Li, N. Biocatalytic upgrading of 5-hydroxymethylfurfural (HMF) with levulinic acid to HMF levulinate in biomass-derived solvents. *ACS Sustainable Chem. Eng.* **2016**, *4*, 4050−4054.

(22) Zhai, S.; Zhang, L.; Zhao, X.; Wang, Q.; Yan, Y.; Li, C.; Zhang, X. Enzymatic synthesis of a novel solid−liquid phase change energy storage material based on levulinic acid and 1,4-butanediol. *Bioresour. Bioprocess.* **2022**, *9*, No. 12.

(23) Malkar, R. S.; Daly, H.; Hardacre, C.; Yadav, G. D. Aldol condensation of 5-hydroxymethylfurfural to fuel precursor over novel aluminum exchanged-DTP@ZIF-8. *ACS Sustainable Chem. Eng.* **2019**, *7*, 16215−16224.

(24) Hafizi, H.; Walker, G.; Iqbal, J.; Leahy, J. J.; Collins, M. N. Catalytic etherification of 5-hydroxymethylfurfural into 5-ethoxymethyfurfural over sulfated bimetallic SO_4^{2-}/Al-Zr/KIT-6, a Lewis/Brønsted acid hybrid catalyst. *Mol. Catal.* **2020**, *496*, No. 111176.

(25) Elsayed, I.; Jackson, M. A.; Hassan, E. B. Catalytic hydrogenation and etherification of 5-hydroxymethylfurfural into 2-(alkoxymethyl)-5-methylfuran and 2,5-bis(alkoxymethyl)furan as potential biofuel additives. *Fuel Process. Technol.* **2021**, *213*, No. 106672.

(26) Tonutti, L. G.; Dalla Costa, B. O.; Mendow, G.; Pestana, G. L.; Veizaga, N. S.; Grau, J. M. Etherification of hydroxymethylfurfural with ethanol on mesoporous silica catalysts of regulated acidity to obtain ethoxymethylfurfural, a bio-additive for diesel. *Microporous Mesoporous Mater.* **2022**, *343*, No. 112145.

(27) Frost, J.; Hellier, P.; Ladommatos, N. A systematic study into the effect of lignocellulose-derived biofuels on the combustion and emissions of fossil diesel blends in a compression ignition engine. *Fuel* **2022**, *313*, No. 122663.

(28) Rahiman, M. K.; Santhoshkumar, S.; Subramaniam, D.; Avinash, A.; Pugazhendhi, A. Effects of oxygenated fuel pertaining to fuel analysis on diesel engine combustion and emission characteristics. *Energy* **2022**, *239*, No. 122373.

(29) Bhat, N. S.; Hegde, S. L.; Dutta, S.; Sudarsanam, P. Efficient Synthesis of 5-(Hydroxymethyl)furfural Esters from Polymeric Carbohydrates Using 5-(Chloromethyl)furfural as a Reactive Intermediate. *ACS Sustainable Chem. Eng.* **2022**, *10*, 5803−5809.

(30) Jarussophon, S.; Pongwan, P.; Srikun, O. Benzoxazinone Intermediate for the Synthesis of Deferasirox. Preparation of Deferasirox. *Org. Prep. Proced. Int.* **2015**, *47*, 483−489.

(31) Vipavanich, C.; Chuepeng, S.; Skullong, S. Heat release analysis and thermal efficiency of a single cylinder diesel dual fuel engine with gasoline port injection. *Case Stud. Therm. Eng.* **2018**, *12*, 143−148.

(32) Tongroon, M.; Chuepeng, S. Adjacent combustion heat release and emissions over various load ranges in a premixed direct injection

diesel engine: A comparison between gasoline and ethanol port injection. *Energy* **2022**, *243*, No. 122719.

(33) Nilaphai, O.; Komanee, K.; Chuepeng, S. Expansion heat release and thermal efficiency of acetone-butanol-ethanol-diesel blended fuel (ABE20) combustion in piston engine. *Fuel* **2022**, *309*, No. 122214.

(34) Chuepeng, S.; Komintarachat, C. Interesterification optimization of waste cooking oil and ethyl acetate over homogeneous catalyst for biofuel production with engine validation. *Appl. Energy* **2018**, *232*, 728−739.

(35) Nilaphai, O.; Hespel, C.; Chanchaona, S.; Mounaïm-Rousselle, C. Spray and combustion characterizations of ABE/dodecane blend in comparison to alcohol/dodecane blends at high-pressure and high-temperature conditions. *Fuel* **2018**, *225*, 542−553.

(36) Rajesh Kumar, B.; Saravanan, S.; Rana, D.; Nagendran, A. Use of some advanced biofuels for overcoming smoke/NO$_x$ trade-off in a light-duty DI diesel engine. *Renewable Energy* **2016**, *96*, 687−699.